Space-time characteristics of diurnal variation in convection and precipitation over the Tibetan Plateau during the Summer Monsoon

***Hatsuki Fujinami[1, 2], Shigeyuki Nomura[3] and Tetsuzo Yasunari[1]**
(1: HyARC, Nagoya University, 2: JST/ CREST, 3: Japan Weather Association)
*** HyARC, Nagoya University, Japan, 464-8601, Furo-cho,**
Chikusa Nagoya, Japan. e-mail: hatsuki@hyarc.nagoya-u.ac.jp

Abstract

We focused on the time-space characteristics of diurnal cycle of convection over the mountain-valley complex terrain in the southern part of the plateau for the transition from noon to midnight. Data used in this study are GMS-IR (0.05 x 0.05 grid) and TRMM PR (0.05 x 0.05 grid) for the summer (JJAS) from 1998 to 2002. Composite diurnal cycle of convection showed that active convection area moves from the mountain ranges (along 28.5N and 30.5N) to valley area (along 29N) from 09 to 18 GMT (from 15 to 00 LST at 90E). This progress was also confirmed in precipitation fields observed by TRMM.

Keyword: Tibetan Plateau, convection, precipitation, diurnal variation, topography.

1. Introduction

Diurnal variation of convection is a prominent phenomenon over the Tibetan Plateau during the northern summer (e.g., Murakami 1983; Fujinami and Yasunari 2001). Some previous studies have shown the relationship between convection and topography over the plateau during summer. Convection (or precipitation) prevails over the mountain ranges in the afternoon, while it is enhanced over the valley in the night over the southern part of the plateau (85°–95°E, 27°–33°N) (Ueno 1998; Kurosaki and Kimura 2002). The major mountain ranges and major valleys over the region are aligned east-west direction (c.f. Fig. 1). The width of mountain ranges is about 100–300 Km, which is very effective topographic scale for water vapor transport by thermally-induced circulation as predicted by a numerical model (Kuwagata et al. 2001).

In this study, we focused on the time-space characteristics of diurnal cycle in convection over the mountain-valley complex terrain for the transition from noon to midnight during summer.

2. Data

We mainly used GMS-IR Tbb data of 0.05° grids as a proxy for cloud activity. Cloud index (*Ic*) is defined as *Ic* = 260-Tbb(K) if 260-Tbb(K) is positive; Ic = 0 if 260-Tbb is negative. Threshold value of 230K is also used to detect high clouds. Cloud-cover frequency (CCF) is also defined as the percentage of cloud cover ($Ic \geq 1$) times to the total number of available data for each grid at each hour. TRMM-PR data (2A25) were also used for the analysis of precipitation. We made 0.05 x 0.05 dataset of PR data. To examine atmospheric circulation fields, we used GAME reanalysis version 1.5 on 0.5° x 0.5° grid in this study. Analysis period in Tbb and game reanalysis is from July to August 1998. In TRMM PR, data for the period from 1998 to 2002 (5 years) were used.

3. Results

Figure 2 shows the spatial distribution of CCF at 09 GMT (15 LST at 90°E) and 15 GMT (21LST) for August 1998. Zonally-elongated areas of high CCF appear along 30.5°N and 28.5°N at 09 GMT (15 LST), which

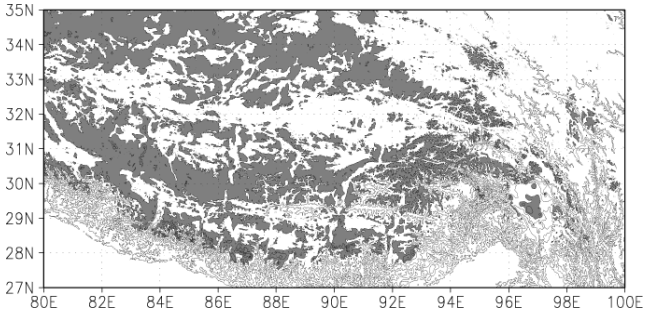

Fig. 1: Topography of the southern part of the Tibetan Plateau. The contour interval is 1,000m. Shading denotes areas higher than 5,000m.

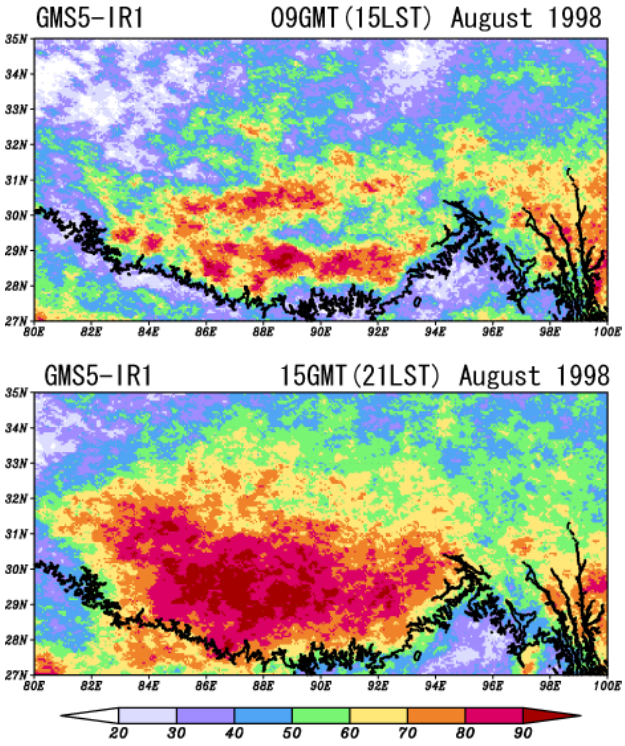

Fig.2: Cloud-cover frequency (%) at 15LST (upper) and 21LST (bottom) in August 1998. The 3,000m topographic contour is shown as a solid line.

correspond to areas of major mountain ranges (see Fig. 1). By contrast, at 21LST (Fig.2-bottom), highest CCF is observed over a wide region centered at valley area along about 29.5°N. The relationship between convections and topography is not clear to the north of 32°N. In order to examine the time evolution of CCF associated with the topography in detail, the latitude-time section of composite diurnal cycle in CCF along 90°E is shown in Fig. 3. CCF becomes higher at around 8–9 GMT (14–15 LST) over the mountain ranges (28.5°N and 30.5°N) and reaches its maximum at 11–12 GMT (17–18 LST). The high CCF area moves from the mountain ranges to valley area (along 29.5°N), and then stays from 13 to 18 GMT (19 to 00 LST). Figure 4 displays a typical case of diurnal variation in convection on 13 August 1998. At 09 GMT (15LST), meso-β (a few 10 Km) scale convective clouds develop over the mountain ranges. The convections grow and combine to extend at 12 GMT (18LST). By 15 GMT (21LST), the convections move and develop into convective cells of about 100 Km over the valley area. Throughout the sequence, convection systems move eastward because the westerly is dominated in the middle through upper troposphere on this day. Circulation fields for 13 August 1998 are shown in Fig. 5. At 200hPa, a deep trough is located along 93°E to the north of 32°N. A center of Tibetan high is observed around 82°E, 28°N. The upper-level westerly is dominated to the north of 28°N over the plateau. In 500 hPa, to the east of 95°E, northwesterly wind prevails north of 32°N, while southwesterly flow is dominant south of 32°N. Over the southern part of the plateau, however, relatively weak synoptic-scale winds are observed, indicating that the atmospheric environment is favorable to induce thermally-driven local circulation.

The characteristics of diurnal variation in clouds are also confirmed in precipitation fields observed by TRMM. Figure 6 indicates the 5-year averaged distribution in precipitation for 06–12GMT (12–18LST) and 12–18GMT (18–00LST) in August. Precipitation amount is lager over the mountain ranges (along about 28.5°N and 30.5°N) during 06–12GMT (12–18LST), while it is enhanced over valley area (along 29.5°N) during 12–18GMT (18–00LST). In the daily mean, precipitation amount is largest over the valley.

References

Fujinami, H. and T. Yasunari, 2001: The seasonal and intraseasonal variability of diurnal cloud activity over the Tibetan Plateau. *J. Meteor. Soc. Japan*, **79**, 1207-1227.

Kurosaki, Y. and F. Kimura, 2002: Relationship between topography and daytime cloud activity around Tibetan Plateau. *J. Meteor. Soc. Japan,* **80**, 1339-1355.

Kuwagata, T., A. Numaguti and N. Endo, 2001: Diurnal variation of water vapor over the central Tibetan Plateau during the summer. *J. Meteor. Soc. Japan,* **79**, 401-418.

Murakami, M., 1983: Analysis of the deep convective activity over the western Pacific and Southeast Asia. Part I: Diurnal variation. *J. Meteor. Soc. Japan*, **61**, 60-76.

Ueno, K., 1998: Characteristics of plateau-scale precipitation in Tibet estimated by satellite data during 1993 monsoon season. *J. Meteor. Soc. Japan*, **76**, 533-548.

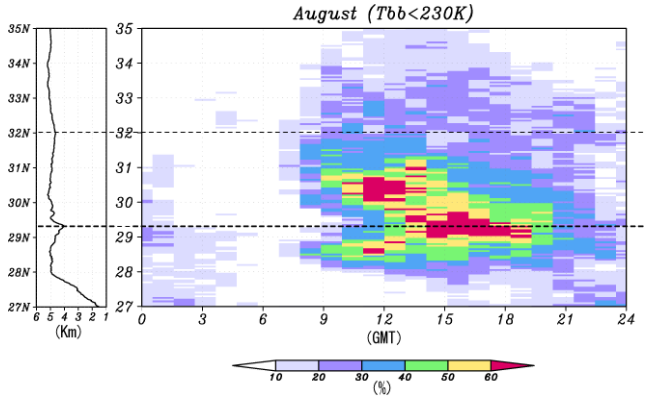

Fig. 3: Latitude-time section of cloud-cover frequency along 90°E. The left side figure indicates the cross section of topography along 90E.

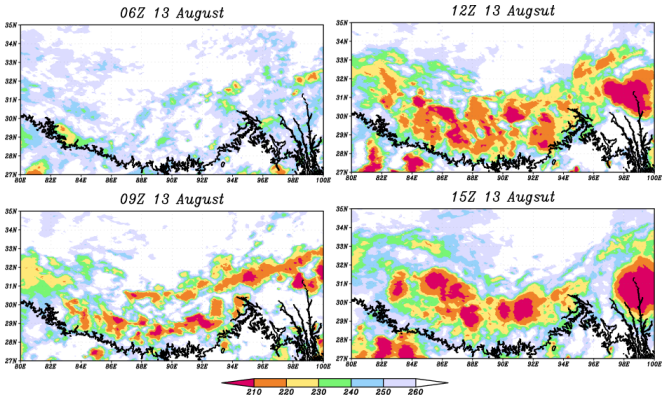

Fig.4: Time evolution of Tbb at 06GMT (12LST), 09GMT (15LST), 12GMT (18LST) and 15GMT (21LST) on 13 August 1998. The 3,000m topographic contour is shown as a solid line.

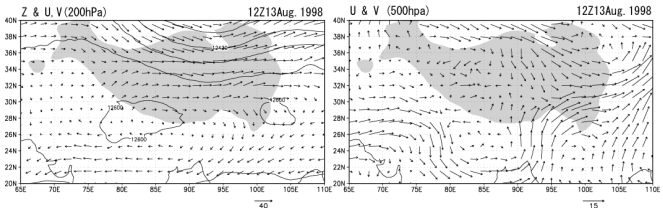

Fig.5 Geopotential height and wind fields at 200 hPa (upper) and wind fields at 500 hPa (bottom) on 12GMT (18LST) 13 August 1998. Shading denotes the Tibetan Plateau.

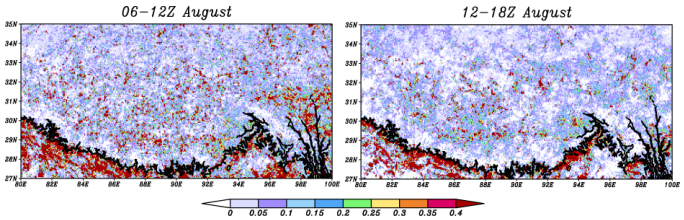

Fig.6 Distribution of 5-year averaged (1998–2002) precipitation for 06–12GMT (12–18LST) (left) and 12–18GMT (18–00LST) (right). A unit is mm/hour.